ADSORPTION OF Pb^{2+} ON TRIMETALLIC OXIDE ($MgO-Fe_2O_3-CuO$) NANOCOMPOSITE COMBINATION WITH GRAPHENE

Received 10-05-2024

Nguyen Kim Thuy, Nguyen Thi Nang, Nguyen Thi Thu, Nguyen Thi Dung, Nguyen Thi Hoai Phuong*

Joint Vietnam-Russia Tropical Science and Technology Research Center

*Email: hoaiphuong1978@gmail.com

TÓM TẮT

HẤP PHỤ Pb^{2+} TRÊN NANOCOMPOSITE $MgO-Fe_2O_3-CuO$/ GRAPHENE

Vật liệu composite $MgO-Fe_2O_3-CuO$/GNPs được tổng hợp bằng phương pháp đồng kết tủa từ muối kim loại kết hợp với thủy nhiệt trên nền GNP. Các đặc tính của vật liệu composite được nghiên cứu, như chụp ảnh SEM, phân tích XRD và EDX. Các tinh thể oxit được phân bố đều trên bề mặt các lớp GNP. Với 26,73% về khối lượng nguyên tố, cacbon có mặt với lượng tương đối lớn trong mẫu composite. Tỷ lệ phần trăm các nguyên tố kim loại (Mg, Fe và Cu) lần lượt là 5,30, 9,24 và 24,21%. Vật liệu cũng được đánh giá khả năng hấp phụ Pb2+ trong dung dịch với dung lượng hấp phụ cực đại là 165,42 mg/g. Mô hình động học bậc hai được ưu tiên hơn mô hình giả bậc nhất. Khả năng hấp phụ tối đa được tính toán bằng mô hình đẳng nhiệt Langmuir của vật liệu composite hỗn hợp oxit ba kim loại trên nền graphene đối với các ion Pb2+ có thể lên tới 1.111 mg/g.

Từ khóa*: oxit hỗn hợp ba kim loại, nanocomposite, graphene, hấp phụ, ô nhiễm chì*

1. INTRODUCTION

One heavy metal element that can be found in nature or produced through a variety of means, such as manufacture and transportation, is lead (Pb). Lead poisoning has a detrimental effect on numerous facets of human health, including the neurological [1], cardiovascular [2], immune system [3], kidney and liver functions [4], etc. More gravely, lead affects fetuses, newborns, and kids in more significant ways, including lower IQ, delayed fetal development, decreased learning capacity, and aberrant behavior [5]. Recent studies have connected lead to fractures, damage, and mutations in DNA. Furthermore, biodiversity is impacted by lead-polluted water supplies, which hinders the growth of plants and animals.

Many methods, such as ion exchange [6], chemical precipitation [7], biological processes [8], etc., have eliminated Pb in water. Adsorption techniques are frequently applied to graphene [9], chitosan [10], alginate [11], etc. Adsorption has many advantages compared to other methods because the materials used as adsorbents are relatively abundant, easy to prepare, inexpensive, and environmentally friendly. Therefore, this is an ongoing issue that many scientists are interested in and researching. In addition to the above materials, metal oxides are also used as Pb adsorbents in aqueous environments

thanks to the electrostatic attraction of oxygen, a highly electronegative element. Metal oxides capable of adsorbing Pb^{2+} ions have been studied, including CuO [12], Fe_2O_3 [13], MnO_2 [14], etc. Furthermore, these oxides are combined with other materials to remove Pb(II) by adsorption, such as MnO_2/PDA [15], Fe_2O_3/chitosan (geopolymer; gelatin) [10], CuO/chitosan/PVA (PANI; cellulose) [16], and other composites. In Vietnam, studies on Pb^{2+} adsorption using agricultural or industrial waste materials have been surveyed and evaluated such as modified red mud, rice husk ash, etc. [17, 18].

Graphene is a one-atom-thick flat sheet of carbon atoms with sp^2 bonds forming a honeycomb-shaped crystal array. In which many graphene sheets are assembled, the C-C bond length in graphene is about 0.142 nm. Graphene is the fundamental structural element of several allotropes, including graphite, carbon nanotubes, and fullerenes. Graphene nanoplatelets are graphene whose main characteristics are easy production, low cost, remarkable electrical and thermal conductivities, excellent mechanical characteristics, a high aspect ratio with a planar shape, and lightweight. They have various applications as fillers for composites, neat coatings, and isolated materials [19]. In some other applications, graphene nanoplatelets are used as a base material for the synthesis of composite materials [20]. In this study, graphene nanoplatelets were used as a base material in manufacturing multi-metal oxide/GNPs composites for Pb^{2+} adsorption in water.

2. EXPERIMENT

2.1. Materials

Graphene nanoplatelets was supplied from VNGraphene Company, Vietnam. $MgCl_2.6H_2O$, $FeCl_3.6H_2O$, $CuCl_2.2H_2O$, and NaOH for co-precipitate were purchased from Macklin, China. Ethanol was bought from Macklin (China) for materials cleaning.

All experiments in this study use original Lead standard solution – $Pb(NO_3)_2$ 1000 mg/L from Merck, USA (code: 1.19776.0500).

2.2. Synthesis of trimetallic oxide/GNPs composite

Mg-Fe-Cu binary oxide/GNPs composite was fabricated by one-pot hydrothermal process. First, $MgCl_2.6H_2O$, $FeCl_3.6H_2O$, and $CuCl_2.2H_2O$ with weight ratio 5:5:5 was dissolved in 80 ml ethanol. Then, 1 g of GNPs was dispersed in mixture by ultrasonic for 15 minutes and stirring for 30 minutes. Final, a 2M NaOH solution was added slow into mixed solution under stirring condition until a pH of 9 was reached. After an hour of stirring, the reaction mixture was transferred in autoclave and heated to 150 °C for 3 hours. Finished reaction, the precipitate was filtered and washed with ethanol/water (volume ratio 1/1) at least three times to remove excess material. The sample was dried at 80 °C in air for 8 hours.

2.3. Characterization

The trimetallic oxide/GNPs composite was characterized by using X-ray diffraction (XRD) on X'Pert Pro, scanning electron microscope (SEM) on Hitachi S-4800, and transmission electron microscopy (TEM) on EMLab NIHE. The porosity of materials was investigated by the N_2 gas adsorption isotherm method on Micromeritics TriStar II device.

2.4. Removal of ion Pb^{2+}

Pb^{2+} contaminated mock water samples were prepared at a concentration of 100 ppm. The experiments were conducted with the ratio of composite to the amount of Pb^{2+} solution of 0.25 g/L. The material

and the Pb^{2+} solution were put into a dark glass vase. In the experiments, the solution was filtered from the sample after 24 hours of adsorption and tested for Pb^{2+} concentration using the Inductively Coupled Plasma (ICP) technique. Before testing, the sample solutions are diluted with the suitable dilute factor.

Adsorption kinetics: A standard experiment involved mixing 100 mL of 30 ppm Pb^{2+} with 25 mg of adsorbent in a glass vessel. The combined solution was agitated at 160 rpm using an orbital shaker. The mixture was filtered, and Pb^{2+} was measured at predetermined intervals. First- and second-order kinetic models were used to investigate the material's adsorption kinetics.

Adsorption isotherm: 100 mL of Pb^{2+} solution with starting concentrations ranging from 10 to 50 ppm was mixed with 25 mg of composite in glass jars. The adsorption process was run for 24 hours at room temperature with 160 rpm shaking. The mixes underwent filtration, and inductively coupled plasma spectrometry (ICP) was utilized to assess any remaining Pb^{2+}. The interaction between the adsorbent and adsorbate is investigated using the Langmuir, Freundlich, and Temkin isotherm equations.

3. RESULTS AND DISCUSSION

3.1. Characterization of trimetallic oxide/GNPs composite

Using the images displayed in Figure 1, scanning electron microscopy (SEM) and transmission electron microscopy (TEM) were used to examine the morphology of the MgO-Fe_2O_3-CuO/GNPs material. With a thickness of less than 20 nm and a diameter of tens of microns, the resulting GNPs exhibit a thin, layered morphology. Additionally, Cu-Fe-Mg oxide crystals were found inside the small spaces between the GNP layers, as seen by the TEM image in Figure 1b. It is clear from the SEM and TEM images of the MgO-Fe_2O_3-CuO/GNPs material in Figure 1 that mixed MgO-Fe_2O_3-CuO oxide was produced and uniformly dispersed on the surface of narrow multilayer graphene. TEM pictures of the composite material reveal that the oxides on the graphene are a mixture consisting of an aggregation of amorphous crystals rather than well-defined nanocrystals.

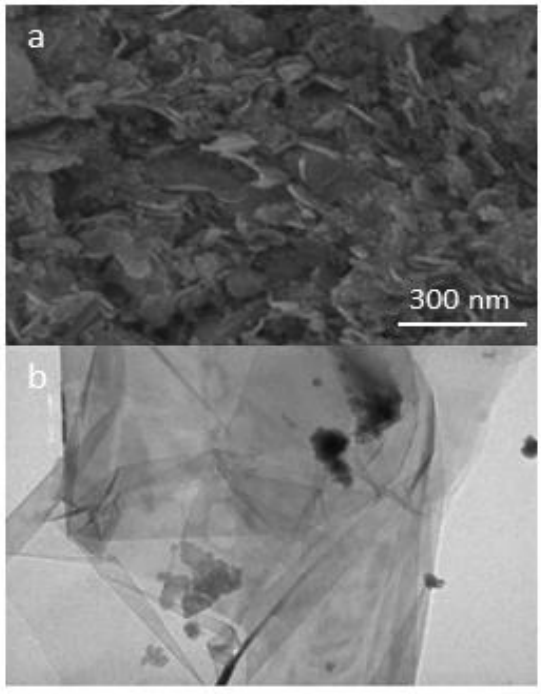

Figure 1. The SEM (a) and TEM (b) images of MgO-Fe_2O_3-CuO/GNPs composite

The X-ray diffraction (XRD) technique confirmed the amorphous nature of the oxide mixture on GNPs, with the results shown in Figure 2a. In the XRD diagram, shallow peaks in the region from 20 to 70 show the amorphous nature of MgO-Fe_2O_3-CuO oxides. At the same time, the combinatorial distribution of oxides on the graphene nanoplatelet surface leads to the masking of the background material. The characteristic peak of GNP was not shown on the diagram. However, in the results of analyzing the elemental content

of the composite sample, the existence of carbon is relatively high at 26.73% by weight. The metal elements (Mg, Fe, and Cu) content reached 5.30, 9.24, and 24.21%, respectively. Meanwhile, the elemental oxygen content is 34.53%, demonstrating the existence of metal oxides in the composite.

3.2. Determine Pb^{2+} concentration in sample solutions by ICP-MS

Determine Pb^{2+} concentration using the ICP-MS system (Thermo Scienctific iCAP RQ ICP-MS)...

Calibration curve is created from 4 level concentrations of Pb^{2+} (100, 200, 500, 1000 µg/L). The results is shown in Figure 3.

The calibration has correlation coefficient value – R^2 = 0.9999. It means that the calibration is excellent to use to determine the concentration of Pb^{2+} in solutions.

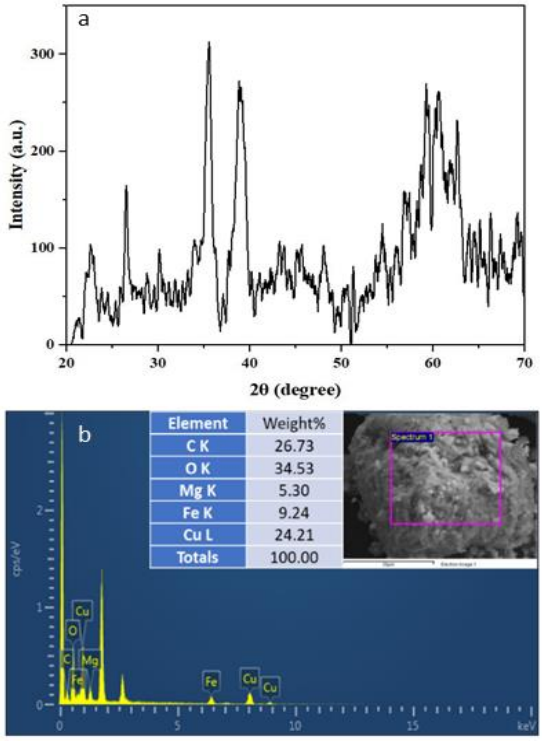

Figure 2. The EDX (a) and XRD (b) patterns of MgO-Fe_2O_3-CuO/GNPs composite

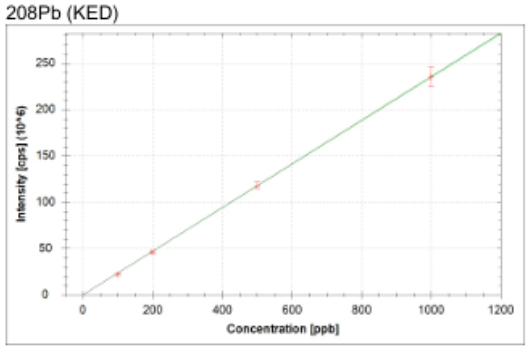

Figure 3. Calibration of Pb^{2+} by iCAP RQ ICP-MS

3.3. Ion Pb^{2+} adsorption of trimetallic oxide/GNPs composite

The kinetics of the adsorption process were evaluated through two apparent kinetic models: first-order and second-order. Based on experimental data on Pb^{2+} adsorption capacity over time, a linear regression of $\ln(q_e-q_t)$ values against t according to the equation of the first-order apparent model, and the following values: $(1/q_t)$ versus t according to the equation of the second-order apparent model. From the slope values and the intersection with the vertical axis of the linear lines, the kinetic constants k_1 and k_2 will be calculated. The linearity of both experimental values according to the model is evaluated by the reliability coefficient R^2. The results of kinematic parameters and reliability coefficients are presented in Table 1.

Table 1. Parameters of the apparent kinetic equation for Pb^{2+} adsorption on MgO-Fe_2O_3-CuO/GNPs material

Pseudo-first-order model			
R^2	k_1 (hour^{-1})	$q_{e,cal}$ (mg/g)	
0.9789	2.4674	59.537	
Pseudo-second-order model			
R^2	$k_2.10^4$ (g/mg. h)	$q^2_{e,cal}$ (mg/g)	$q^2_{e,exp}$ (mg/g)
0.9984	0.0506	111.11	99.52

The results in Table 1 show that the pseudo-second-order model is more reliable than the pseudo-first-order model. Furthermore, the equilibrium adsorption capacity value is obtained from the experiment, and the equation calculates the value. There is a significant difference in the pseudo-first-order equation, while this result is equivalent to the value calculated according to the pseudo-second-order equation. From there, it can be seen that the Pb^{2+} adsorption process by MgO-Fe_2O_3-CuO/GNPs material follows according to the pseudo-second-order model.

This study analyzed data using Langmuir, Freundlich, Temkin, Redlich-Peterson, and Dubinin-Radushkevich models. The following formula gives the linear equation of the Langmuir isotherm model:

$$\frac{1}{q_e} = \frac{1}{q_m} + \frac{1}{K_L \cdot q_m} \cdot \frac{1}{C_e}$$

$$R_L = \frac{1}{1 + K_L C_0}$$

The following formula expresses the linear equation of the Freundlich isotherm model:

$$lnq_e = lnK_F + \frac{1}{n} lnC_e$$

The equation represents the Temkin isotherm model:

$$q_e = \beta lnK_T + \beta lnC_e$$

The Redlich-Peterson isothermal model has three unknown parameters and is represented by the formula:

$$ln\left(K_{RP}\frac{C_e}{q_e} - 1\right) = \beta lnC_e + \beta ln\alpha_{RP}$$

The equation expresses the linear form of the Dubinin-Radushkevich isotherm model:

$$lnq_e = lnq_m - \beta\varepsilon^2$$

In which: $\varepsilon = RT\ ln\left(1 + \frac{1}{C_e}\right)$

The average adsorption energy value indicates the nature of the adsorption process. When the E value is less than 8 kJ/mol, the adsorption process is physical, and 8 - 16 kJ/mol is chemical adsorption. The average adsorption energy can be calculated from the Dubinin - Radushkevich model according to the formula:

$$E = \frac{1}{\sqrt{-2\beta}}$$

The isotherm parameters are given in Table 2.

Table 2. Parameters of Pb^{2+} adsorption isotherms using MgO-Fe_2O_3-CuO/GNPs material.

Model	**Parameters**	
Langmuir	K_L	1.00
	q_m (mg/g)	1,111.1
	R^2	0.9981
Freundlich	1/n	0.577
	K_F	346.71
	R^2	0.916
Tempkin	K_T	27.39
	b_T (kJ.mol)	0.014
	R^2	0.9672
Redlich-Peterson	K_R	2562.2
	α_R (L/mg)	4.754
	β	0.781
	R^2	1
Dubinin – Radushkevich	E (kJ/mol)	0.141
	β	25.005
	R^2	0.972

From Table 2, the results show that the isotherms Langmuir, Freundlich, Temkin, Redlich-Peterson, and all Dubinin - Radushkevich have high R2 coefficients (R^2 > 0.91), Especially for the Redlich-Peterson isotherm, the coefficient R^2 = 1.

The value of Temkin's constant: b_T - typical for the heat of adsorption of Pb^{2+} ion is 0.014 kJ/mol. The slight heat of the adsorption value shows a weak interaction between the adsorbent and the adsorbent. The average adsorption energy value calculated according to the Dubinin - Radushkevich model: E = 0.141 < 8 kJ/mol shows that the adsorption process is physical adsorption. Calculation results according to the Langmuir isotherm model show that the maximum adsorption capacity for Pb^{2+} reaches a high value of 1,111 mg/g, showing the material's potential for Pb^{2+} ion adsorption.

4. CONCLUSION

Research results show that the MgO-Fe_2O_3-CuO/GNPs material can adsorb Pb^{2+} in solution with an adsorption capacity of 165.42 mg/g. Optimal conditions for Pb^{2+} adsorption include an initial concentration of 20 mg/l, a material ratio of 0.1 g/l, and a treatment time of 2 hours. The maximum adsorption capacity calculated according to the Langmuir isotherm model of the composite material of mixed oxides on a narrow multilayer graphene substrate for Pb^{2+} ion can be up to 1,111 mg/g. This proves that the potential of the synthesized material to remove Pb^{2+} in water is very high.

Acknowledgments: This work is supported by Joint Vietnam-Russia Tropical Science and Technology Research Center.

Declaration: The authors declare that this is the work of our and this content has not been submitted to any journal.

REFERENCES

[1] Natalia Pozdnyakova, N. K., Artem Pastukhov, (2024). Multipollutant reciprocal neurological hazard from smoke particulate matter and heavy metals cadmium and lead in brain nerve terminals. *Food and Chemical Toxicology*, **185**, 114449.

[2] Brooks B. Gump, D. T. H., (2023). Perfluoroalkyl substances (PFAS) and lead (Pb) as “cardiovascular disruptors” in 9–11-year-old children living in Syracuse, New York, United States. *Environmental Research*, **236**, 116758.

[3] Mishra, K. P., (2009). Lead exposure and its impact on immune system: A review. Toxicology in Vitro, 23, 969–972.

[4] Vesna Matovic´, A. B., Danijela Đukic´ - C´ osic´, (2015). Zorica Bulat, Insight into the oxidative stress induced by lead and/or cadmium in blood, liver and kidneys. *Food and Chemical Toxicology*, **78**, 130-140.

[5] Axelrad, D. A.; Coffman, E.; Kirrane, E. F.; Klemick, H., (2022). The relationship between childhood blood lead levels below 5 microg/dL and childhood intelligence quotient (IQ): Protocol for a systematic review and meta-analysis. Environ Int, **169**, 107475.

[6] Yaqin Rong, W. Y., Zhongde Wang, Xiaogang Hao, Guoqing Guan, (2023). Rapid and selective removal of Pb ions by electroactive titanium Dioxide/Polyaniline ion exchange film Separation and Purification Technology, **312**, 123386.

[7] Haojie Chen, R. X., Danlian Huang, Rui Deng, Ruijin Li, Yashi Chen, Wei Zhou, (2024). Three kinds of apatite adsorbents prepared by co-precipitation for Pb (II) and Cd (II) removal from wastewater: performance, competitive effects and mechanisms. *Journal of Molecular Liquids*.

[8] Yuzhu Yang, A. A., Junfeng Su, Liang Xu, Xumian Wang, Enlei Liang, (2022). Simultaneous removal of nitrate, tetracycline, and Pb(II) by iron oxidizing strain Zoogloea sp. FY6: Performance and mechanism. *Bioresource Technology*, **360**, 127569.

[9] Kuganathan, N.; Anurak Avan, S.; Abiman, P.; Ingrain, P.; Gansa, E. I.; Chroneos, A., (2021). Adsorption of lead on the surfaces of pristine and B, Si and N-doped graphene. *Physica B: Condensed Matter*, **600**, 412639.

[10] Liu, X.; Wang, Y.; Wu, X.; Wang, Y.;

Fan, G.; Huang, Y.; Zhang, L., (2024). Preparation of magnetic DTPA-modified chitosan composite microspheres for enhanced adsorption of Pb(II) from aqueous solution. *Int J Biol Macromol*, **264(Pt 1)**, 130410.

[11] Alavinia, S.; Ghorbani-Vaghei, R.; Asad Abadi, S.; Atrian, A., (2023). Sodium alginate/diethyleneamine-triazine-sulfonamide nanocomposite for adsorptive removal of Pb(II) and methyl violet from aqueous solutions. *Materials Chemistry and Physics*, **293**, 126915.

[12] Arfaoui, L.; Kouass, S.; Dhaouadi, H.; Jebali, R.; Touati, F., (2015). Characterization and adsorption performance of Pb(II) on CuO nanorods synthesized by the hydrothermal method. *Materials Research Bulletin*, **70**, 284-290.

[13] Wang, H.; Sun, W.; Liang, X.; Zou, H.; Jiao, X.; Lin, K. A.; Li, T., (2021). Two-dimensional Fe_2O_3 nanosheets as adsorbent for the removal of Pb(II) from aqueous solution. *Journal of Molecular Liquids*, 335, 116197.

[14] Lin, M.; Chen, Z., (2020). A facile one-step synthesized epsilon-MnO_2 nanoflowers for effective removal of lead ions from wastewater. *Chemosphere*, **250**, 126329.

[15] Li, X.; Zhao, Y.; Wang, D.; Du, X., (2023). Dual-propelled PDA@MnO_2 nanomotors with NIR light and H_2O_2 for effective removal of heavy metal and organic dye. *Colloids and Surfaces A: Physicochemical and Engineering Aspects*, **658**, 130712.

[16] Jiao, X.; Gutha, Y.; Zhang, W., (2017). Application of chitosan/poly(vinyl alcohol)/CuO (CS/PVA/CuO) beads as an adsorbent material for the removal of Pb(II) from aqueous environment. *Colloids Surf B Biointerfaces*, **149**, 184-195.

[17] Lợi, V.Đ., D.T. Hưng, and N.T. Vân, (2015). Nghiên cứu khả năng hấp phụ chì (Pb) trong dung dịch từ bùn đỏ biến tính. Tạp chí phân tích Hóa, Lý và Sinh học, **20(4)**, 117-129.

[18] Nguyen, T.B., et al., (2023). Trấu, than hoạt tính, Than hoạt tính từ vỏ trấu: tổng hợp, đặc trưng và ứng dụng trong hấp phụ Cr (III) và Pb (II) từ dung dịch nước. *Hue University Journal of Science: Natural Science*,**132(1A)**, 83-93.

[19] Łukawski, D.; Hochmańska-Kaniewska, P.; Bałęczny, W.; Martin, A.; Janiszewska-Latterini, D.; Lekawa-Raus, A., (2024). Phenol-formaldehyde resin enriched with graphene nanoplatelets as an electroconductive adhesive for wood composites. *International Journal of Adhesion and Adhesives*, **132**, 103678.

[20] Niavol, S. S.; Khatibani, A. B.; Moghaddam, H. M.; Gao, G., (2024). ZnO quantum dots decorated on graphene oxide and graphene nanoplatelets: Comparison the structure and sensing properties. *Inorganic Chemistry Communications*, **16**, 111957.